IOP PUBLISHING EUROPEAN JOURNAL OF PHYSICS

Eur. J. Phys. **30** (2009) 75–84 doi:10.1088/0143-0807/30/1/008

Dynamic soaring: aerodynamics for albatrosses

Mark Denny

5114 Sandgate Road, RR#1, Victoria, British Columbia, V9C 3Z2, Canada

E-mail: markandjane@shaw.ca

Received 27 August 2008, in final form 1 October 2008
Published 6 November 2008
Online at stacks.iop.org/EJP/30/75

Abstract

Albatrosses have evolved to soar and glide efficiently. By maximizing their lift-to-drag ratio L/D, albatrosses can gain energy from the wind and can travel long distances with little effort. We simplify the difficult aerodynamic equations of motion by assuming that albatrosses maintain a constant L/D. Analytic solutions to the simplified equations provide an instructive and appealing example of fixed-wing aerodynamics suitable for undergraduate demonstration.

1. Introduction

Albatrosses (figure 1) are among the most pelagic of birds. They nest on remote islands in the 'Roaring Forties' and 'Furious Fifties', i.e., in the wind-swept southern regions of the Pacific, Atlantic and Indian Oceans that surround Antarctica. They feed primarily upon squid, and roam widely for food to feed their young. A typical albatross feeding trip may take 10 days and cover 1000 km per day. Albatrosses may make half a dozen circumpolar trips each year, taking advantage of the prevailing westerly winds, and adopting characteristic looping flight patterns that best extract energy from the wind. When travelling northward they loop in an anticlockwise direction, and loop clockwise when heading south (we will explain why this is so).

Albatrosses are supremely well adapted to this pelagic[1] life in the windy southern oceans. They are able to sleep on the ocean surface. They have a unique 'shoulder lock' skeletal adaptation that permits them to maintain their wings outstretched with little effort. Those wings are made for gliding and soaring, rather than flapping flight; they are very long (the wings of the Wandering Albatross, *Diomedea exulans*, are the longest of any living bird, at 3.5 m) and thin, with a large aspect ratio of about 16. Such wings are capable of producing a ratio of lift-to-drag forces of $L/D = 25$; this is much greater than the ratio attained by other birds. (Even that consummate flier the common tern has an L/D ratio that is only half that of the albatrosses.) The large value of L/D permits an albatross to glide and soar over long

[1] Adults nest every second year and spend the rest of their time at sea. Juveniles that have left their nest may not set foot on land for 7–10 years.

Figure 1. A pair of black-browed albatrosses. Note the streamlined bodies and slender wings, a combination that provides a large lift-to-drag ratio. (Photo courtesy of Wim Hoek.)
(This figure is in colour only in the electronic version)

distances without any effort; they are able to fly for hours—and even make headway against the wind—without once flapping their wings. Such flight requires very little energy: the heart rate of a soaring albatross is only slightly higher than its basal rate when resting on land [1–3].

Great progress has been made, over the last 30 years, in understanding the physics of bird flight. Flapping flight is, of course, much more difficult to describe quantitatively than the well-understood (though mathematically complex) aerodynamics of fixed-wing airplanes [4–7]. We might expect that soaring bird flight will be less difficult to understand; indeed a number of studies have been made [8, 9]. Even these, however, may be considered dauntingly complicated by an undergraduate student. There are a large number of parameters that a flying bird can vary (such as drag coefficient, wing aspect ratio, wing area, camber and taper) which are more or less fixed for airplanes. We can turn this added complexity into a simplifying and reasonable assumption for an albatross flight analysis, however. In this paper, we assume that albatrosses control their wing camber, taper, etc, so as to maintain a constant (usually the maximum) value for L/D. We will show that this assumption reduces the flight equations of motion to a simple differential equation that is straightforward to solve analytically in many cases of interest. The resulting predictions yield an insight into albatross flight dynamics in a manner that is accessible to undergraduates.

2. Equation of motion

The velocities and forces relevant to our airborne albatross are shown in figure 2. Note that the components of ground speed $u_{x,z}$ are related to air speed v via

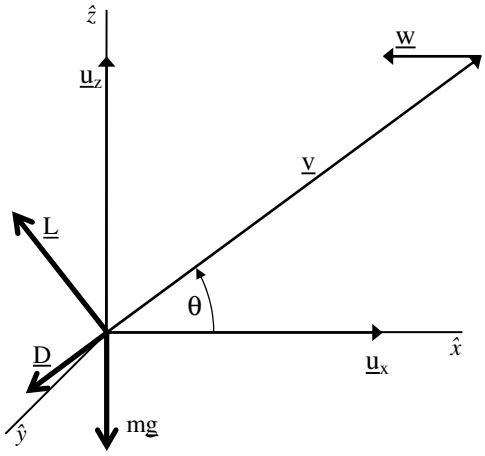

Figure 2. Relevant velocities (thin arrows) and forces (thick arrows) describing albatross flight. The velocities $\underline{u}_{x,z}$ are measured relative to the ground, whereas $\underline{v}$ is measured relative to the air (so that $u = \sqrt{u_x^2 + u_z^2}$ is the ground speed and v is the air speed). Wind velocity is $\underline{w}$, and so $\underline{u}_x + \underline{u}_z = \underline{v} + \underline{w}$. Lift and drag force vectors are $\underline{L}$, $\underline{D}$; the albatross weight is mg.

$$u_z = v\sin(\theta), \qquad u_x = v\cos(\theta) + w. \tag{1}$$

where w is wind speed. We assume that the wind moves horizontally ($\underline{w} = w\hat{x}$, where $\hat{x}$ is a unit vector along the x-direction) and that the speed is not constant, but increases with height z above the ocean surface:

$$w = -\alpha z. \tag{2}$$

(The minus sign indicates that the albatross is moving into the wind, as illustrated in figure 2; for a tailwind w is positive.) This wind shear is due to friction with the ocean surface and the boundary layer, within which equation (2) applies, and is assumed to extend to an altitude $h = 20$ m. Above this altitude the wind speed is assumed to be independent of height. Such a linear wind speed profile is a simplification of the observed profile (which is logarithmic), but is convenient for calculation. From figure 2 we can write, for the horizontal and vertical components of force that act upon the albatross:

$$-L\sin(\theta) - D\cos(\theta) = m\dot{u}_x, \tag{3a}$$

$$L\cos(\theta) - D\sin(\theta) - mg = m\dot{u}_z. \tag{3b}$$

Here we are assuming that the wind and albatross velocity vectors are in the same plane, so that the problem we address is two dimensional. Substituting from equations (1) and (2) and noting that $\dot{z} = u_z = v\sin(\theta)$, we obtain for the lift and drag forces:

$$L = mg\cos(\theta) + mv\dot{\theta} + mv\alpha\sin^2(\theta), \tag{4a}$$

$$D = -mg\sin(\theta) - m\dot{v} + mv\alpha\sin(\theta)\cos(\theta). \tag{4b}$$

Equations (4) apply in the case of a headwind; for a tailwind $\alpha \to -\alpha$.

To obtain the full equations of motion for bird flight, we must express the lift and drag forces L and D as functions of airspeed v. Thus, for example, we usually write $D = av^2 + bL^2/v^2$. Here a is the sum of profile and parasitic drag coefficients (representing

the drag on wings and body, respectively) and b is the induced drag coefficient [4]. Lift may be constant (equal to mg for horizontal flight) but in general it, too, depends upon air speed. The coefficients a and b depend upon morphological factors that are, at least in part, under the bird's control. We use this fact to simplify equations (4) by assuming that our albatross maintains a constant ratio of L/D; let us denote this ratio by k, and adopt a minimum value of $k = 1$ and a maximum value of $k = 25$ for albatross flight[2].

From equations (4) and our assumption $L = kD$ we obtain

$$\dot{v} = -g\left(\sin(\theta) + \frac{1}{k}\cos(\theta)\right) + \left[\alpha\sin(\theta)\left(\cos(\theta) - \frac{1}{k}\sin(\theta)\right) - \frac{1}{k}\dot{\theta}\right]v, \quad (5)$$

again, $\alpha \to -\alpha$ for a tailwind. Equation (5) is relatively easy to work with; in the remainder of this paper, we solve special cases of interest analytically and in so doing obtain an understanding of how albatrosses can fly long distances without expending much energy.

3. Special cases: glide angle, efficiency and equilibrium speed

Firstly let us assume that our albatross is in still air (so that $\alpha = 0$). For a glide along a straight trajectory (constant θ), equation (5) reduces to $\dot{v} = -g\big(\sin(\theta) + \frac{1}{k}\cos(\theta)\big)$ and so a constant equilibrium speed occurs for a dive angle $\theta_{\rm eq}$ given by $\tan(\theta_{\rm eq}) = -1/k$. (Negative θ indicates a descending trajectory; positive θ means ascending, as shown in figure 2.) This well-known result [10] shows that a high L/D (corresponding to a large k) results in a long glide distance; an albatross gliding from a certain height will travel further than other birds gliding from the same height.

Now we consider a rising trajectory in still air with constant $\dot{\theta} \equiv \omega$, so that equation (5) reduces to $\dot{v} = -g\left[\sin(\omega t) + \frac{1}{k}\cos(\omega t)\right] - \frac{\omega}{k}v$. This equation can be solved analytically (via an integrating factor $\exp(\omega t/k)$) to yield for the airspeed:

$$v(t) = \left(v_0 - \frac{g}{\omega}\cos(\eta)\right)\exp\left(-\frac{\omega}{k}t\right) + \frac{g}{\omega}\cos(\omega t + \eta) \qquad \text{where} \quad \sin(\eta) \equiv \frac{2k}{k^2+1}. \quad (6)$$

Let us say that the albatross ascends a height H and in so doing its speed drops from v_0 at $\theta = 0$ to zero at $\theta = \pi/2$. The height H is given by

$$H = \int_0^{\pi/2\omega} {\rm d}t\, v(t)\sin(\omega t). \quad (7)$$

From equations (6) and (7) and from the boundary conditions, it is straightforward to calculate the efficiency of this climbing flight manoeuvre. The bird's initial energy is $E_i = \frac{1}{2}mv_0^2$ and its final energy is $E_f = mgH$. The efficiency is $\varepsilon \equiv E_f/E_i$.

The fractional loss of energy $1-\varepsilon$ for this climbing manoeuvre is plotted in figure 3 as a function of the lift-to-drag ratio, k. Note that, because of their high k value, albatrosses lose much less energy during a climb than do birds with lower lift-to-drag ratios. We can infer from this observation that there is significant selection pressure for albatrosses to evolve high lift-to-drag ratios (because these birds are so dependent upon efficient flight).

Now we consider the equilibrium ($\dot{v} = 0$) speed for the more general case $\alpha \neq 0$. Again we restrict attention to linear trajectories with a constant θ. Equilibrium speed is readily found from equation (5) to be

$$v_{\rm eq} = \frac{g}{\alpha}\frac{\tan(\theta+\phi)}{\sin(\theta)} \qquad \text{where} \quad \tan(\phi) \equiv \frac{1}{k}. \quad (8)$$

[2] Barnes [3] suggests a maximum value of $k = 27$ whereas Alexander and Vogel [11] adopt a somewhat lower figure of $k = 18$. This range of albatross maximum lift-to-drag ratios is high for birds, but is less than can be attained by modern gliders and sailplanes.

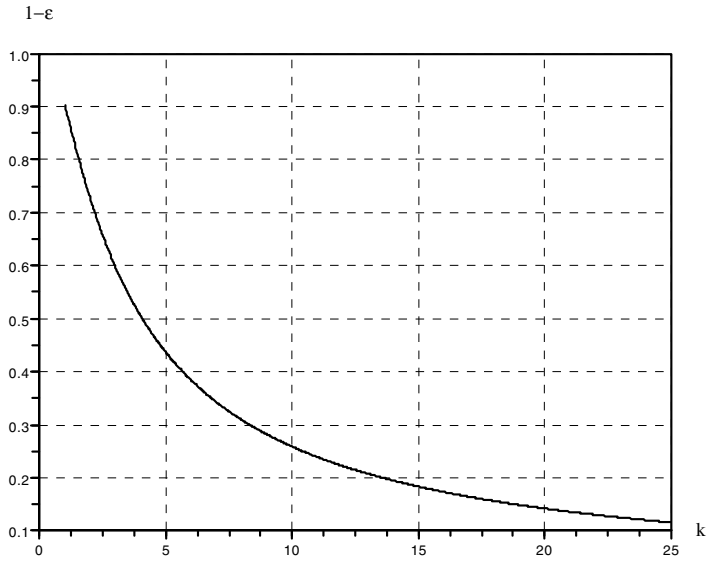

Figure 3. Fraction of albatross energy lost during a climb (described in the text) versus the lift-to-drag ratio k.

Does this speed correspond to stable or unstable equilibrium? Stability requires that the coefficient of v in equation (5) (the term in square brackets) be negative. It is not difficult to show that this requirement, combined with the requirement that speed v be positive[3], means that for the two cases of practical interest (diving in a tailwind and climbing in a headwind) the equilibrium speed is unstable. So an albatross must constantly adjust parameters in order to maintain a constant speed.

4. Rayleigh dynamic soaring

What is special about the two trajectories just mentioned (diving while moving downwind and climbing while moving upwind)? When combined into a single looping trajectory, these constitute dynamic soaring (DS), familiar to every glider pilot. DS permits a glider (or albatross) to extract energy from the wind when there is a vertical velocity gradient, such as the one that occurs in the lee of a hill or on the boundary layer adjacent to the earth's surface. Here we will analyse a simple trajectory that shows how an albatross uses DS to move across the wind, with no net energy expenditure. Rayleigh, in 1883, was the first to suggest that seabirds such as albatrosses might exploit the DS technique [12].

Consider the flight trajectory that is sketched in figure 4. Here we have joined together three two-dimensional trajectories, and so we can apply equation (5) to each segment separately. The albatross begins at the top of the boundary layer (altitude $h = 20$ m) with airspeed $v_{\min} = 12$ m s^{-1}, which we take to be the minimum airspeed that the bird requires to maintain lift [13]. Groundspeed is $v_{\min} + \alpha h$. The first phase of the trajectory consists of a dive at a constant angle θ_1 along the wind direction; the second phase is a long glide at zero altitude; the third phase is a climb at a constant angle θ_3 into the wind, ending at an altitude h

[3] Negative v corresponds to movement to the left, in figure 2, which means that the wind (assumed in figure 2 to be headwind) is a tailwind. Similarly, negative v in a tailwind implies headwind. So, v must be positive.

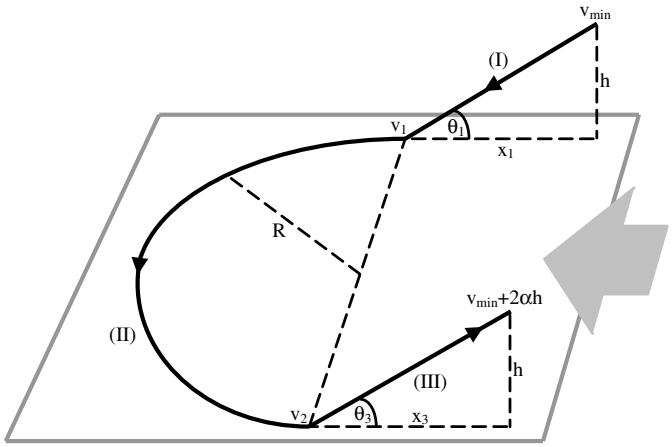

Figure 4. Dynamic soaring model trajectory. Wind is from the right; wind speed increases proportionally with altitude. The three flight phases consist of (I) diving downwind (II) gliding at zero altitude, where there is no wind (III) climbing into the wind. The albatross begins at an altitude h, heading downwind with the air speed $v_{\min}$, and finishes at the same altitude heading upwind with the air speed $v_{\min} + 2\alpha h$. Albatross flight speed relative to the earth's surface is the same at the start and finish ($v_{\min} + \alpha h$), and so the albatross energy at the start and finish is the same. Such zero-energy trajectories are possible. The bird moves a distance $2R$ across the wind, and a distance $x_3 - x_1$ upwind. The diagram shows the trajectory in a frame moving with the wind speed; in a frame fixed to the surface the trajectories of phases I and III are curved.

with the airspeed $v_{\min} + 2\alpha h$ (so that groundspeed is once again $v_{\min} + \alpha h$). Thus the albatross has travelled across the wind a distance $2R$ at a net cost of zero energy. We will show that such a trajectory is possible. This calculation goes a long way towards demonstrating how albatrosses can exploit DS to extract energy from the wind, but it does not quite provide a full explanation, because we have not closed the trajectory: the albatross needs to turn at the end of the third phase, so that it is pointing downwind. This omission and other deficiencies of the simple trajectory of figure 4 are discussed below, where we argue that, in fact, our calculation *underestimates* the energy extracted from the wind.

The virtue of our simple trajectory is that albatross speed during each phase can be calculated readily from equation (5). Thus, for example, phase II begins with the albatross at speed v_1 and ends at speed v_2; the equation of motion reduces to $\dot{v} = -g/k$ (from equation (5), with $\theta = \dot{\theta} = 0$). So, we see why large L/D ratio k helps the bird glide further than would be the case for a small L/D value. Phases I and III are both described by an equation of motion of the form $\dot{v} = a + bv$, where the constants a and b depend upon parameters θ, k and α. There is an additional constraint for phases I and III: $\int \mathrm{d}t\, v(t) \sin(\theta_{1,3}) = h$. All of these equations are trivial to solve. Matching solutions at the boundaries is tedious but straightforward. We leave the detailed solutions to the interested reader, and here will simply summarize the results.

Firstly we note that the parameters are constrained as follows:

$$\cos(\theta_1) + \frac{\sin(\theta_1)}{k_1} + \cos(\theta_3) - \frac{\sin(\theta_3)}{k_3} > 2, \tag{9}$$

where subscripts 1, 3 refer to phases I, III. Parameters that satisfy inequality (9) do not always lead to acceptable solutions; (9) is a necessary but not sufficient condition. From (9), we see that a low value for k_1 is required—the albatross flying in a tailwind benefits from high drag.

We choose $k_1 = 1$. We also see that climb angle should be small, and that the L/D ratio k_3 should be as large as possible. We choose $k_3 = 25$, and we find that a climb angle of $\theta_3 = 15^\circ$ works. The equations of motion show that the trajectory of figure 4 is possible only for steep dive angles; here we choose dive angle $\theta_1 = -60^\circ$.

Calculations show that figure 4 trajectories are possible in moderate to strong winds, with gradients exceeding $\alpha = 0.5\ \mathrm{s}^{-1}$ (which corresponds to wind speeds above the boundary layer of $\alpha h = 10\ \mathrm{m\ s}^{-1}$ or 36 kph). The change in albatross energy during each phase is

$$\Delta E_1 = \tfrac{1}{2}mv_1^2 - mgh - \tfrac{1}{2}m(v_{\min} + \alpha h)^2, \tag{10a}$$

$$\Delta E_2 = \tfrac{1}{2}mv_2^2 - \tfrac{1}{2}mv_1^2, \tag{10b}$$

$$\Delta E_3 = mgh + \tfrac{1}{2}m(v_{\min} + \alpha h)^2 - \tfrac{1}{2}mv_2^2. \tag{10c}$$

Note that energy is determined in a reference frame that is fixed to the earth's surface. The total energy change over the trajectory is zero, in this frame, by construction. The air speeds $v_{1,2}$ apply at the beginning and end of phase II, as shown in figure 4. These speeds are found to be quite high, varying from $v_2 = 29.760\ \mathrm{m\ s}^{-1}$ for $\alpha = 0.5$ to $v_1 = 40.094\ \mathrm{m\ s}^{-1}$ for $\alpha = 0.9$. Solutions in stronger winds (larger α) are possible, at even higher speeds. Albatrosses are certainly capable of such speeds: measurements of one grey-headed albatross during an Antarctic storm showed that the bird travelled for 9 h at ground speeds of between 110 kph ($30.5\ \mathrm{m\ s}^{-1}$) and 168 kph ($46.7\ \mathrm{m\ s}^{-1}$) [14]. The changes in energy for the three phases of the figure 4 trajectory are plotted in figure 5. Energy is gained during the dive (phase I), lost during the zero-altitude glide (phase II) and lost a little during the climb (phase III). This behaviour is easy to understand qualitatively. The albatross is pushed along by the wind during the dive, and so picks up more speed than we would expect simply from the change in altitude. Energy is lost to drag during the horizontal wave-top glide. Perhaps more surprising is the relatively small loss of energy during the climb phase. Here the albatross is gaining height and flying into the wind, and yet it picks up airspeed. Of course, the ground speed falls as the bird rises.

We also plot the albatross cross-wind and upwind speeds in figure 5. These speeds are calculated relative to the surface. So, for example, an albatross that repeatedly flies the DS trajectory of figure 4 in a strong wind gradient of $\alpha = 0.9\ \mathrm{s}^{-1}$ will drift more or less perpendicular to the wind direction at a speed of about $19\ \mathrm{m\ s}^{-1}$. In a gentler gradient of $\alpha = 0.6\ \mathrm{s}^{-1}$, assuming that the bird adopts the same dive and climb angles, the cross-wind speed will be about $9\ \mathrm{m\ s}^{-1}$, while the upwind speed is $8\ \mathrm{m\ s}^{-1}$. By changing dive and climb angles, an albatross can alter its drift direction.

Finally, we note that DS still occurs if the albatross maximum L/D is reduced (to $k = 20$) and the minimum velocity is increased (to $v_{\min} = 15\ \mathrm{m\ s}^{-1}$); the trajectory speed is increased by about $3\ \mathrm{m\ s}^{-1}$, assuming all other parameters are unaltered, and DS requires stronger winds (a minimum value of $\alpha = 0.65\ \mathrm{s}^{-1}$). DS is more severely limited if the minimum L/D is increased: α must exceed $0.85\ \mathrm{s}^{-1}$ if k_1 is increased from 1.0 to 1.5. We may conclude that, for a wide range of parameters, it is possible for albatrosses to exploit the Rayleigh DS in moderate to strong wind conditions.

5. DS model limitations

The central assumptions of our DS model are

(1) constant L/D during each phase of the trajectory,
(2) linear wind speed profile,

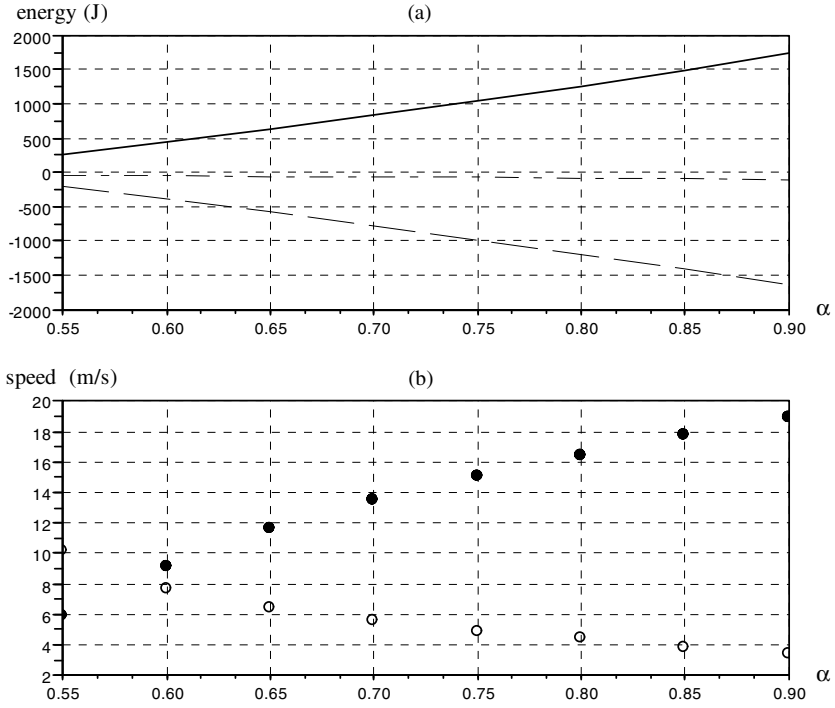

Figure 5. (a) Gain in albatross energy during phase I (solid line), phase II (dashed line) and phase III (dot–dash line) for a bird of mass 11 kg. (b) Albatross speed relative to the earth's surface across the wind (filled circles) and upwind (open circles). In both cases the horizontal axis is wind gradient parameter α (s^{-1}).

(3) transition effects between flight phases are negligible and
(4) wave lift and the ground effect are negligible during phase II.

The first is a plausible hypothesis; for example, it is reasonable to assume during phases II and III that the albatross will maintain L/D as high as possible—evolution has provided it with the capability of exceptionally large L/D, which benefits the bird during these flight phases—and so k is fixed at the maximum value. The second assumption is a mathematical simplification that approximates the actual wind speed profile. Thus the DS model has zero wind speed near the surface and constant speed above the boundary layer, as in the real world; the model predictions that depend upon speed profile will approximate real world observations. Transparency has been attained at the cost of approximation (a statement that could be applied to much of physics).

The third assumption refers to the adjustments in wing shape, angle of attack, etc, that are necessary for the albatross to change flight direction and (between phases I and II) k value. We have assumed that these adjustments do not consume significant energy. This may be reasonable for the transitions between phase I and II, and between II and III, but it is surely not reasonable for the transition between phase III and phase I. During this transition the albatross must turn around, from flying into the wind to flying downwind, at the highest point of the trajectory where wind speed is greatest. We have not modelled this transition because it would be very complicated to do so: the k value and apparent wind direction change during the turn, as does the albatross cross-sectional area that is exposed to the wind. The purpose of

our simple DS model is to demonstrate that an albatross can use the wind energy to move; it can travel large distances without exerting much internal energy. Neglecting the turn between flight phase III and flight phase I does not invalidate this model result, we argue, because the turn will *increase* the albatross energy[4], so that it is easier than predicted here for the albatross to utilize DS. Thus our simple model cannot calculate the turn, and so underestimates the benefits gained by DS.

The fourth assumption is made because modelling the ground effect, and the influence of surface waves upon albatross flight, is complicated. The ground effect (disturbance of wingtip vortices by the ground, or ocean surface, resulting in additional lift) is exploited in several airplane designs. It has also been shown to benefit certain birds (such as skimmers) that fly close to the water surface [15]. The action of waves has been shown to benefit albatross flight: the bird gains thrust while drag is reduced, to an extent that depends in a complicated way upon the surface wave parameters [16]. Thus, once again, ignoring a complication leads to our model underestimating the ability of albatrosses to exploit DS. Thus our simple model predicts a *minimum* DS capability.

6. Summary and discussion

Albatross flight dynamics is of interest beyond the biomechanics community. There is much research today into micro air vehicles (MAVs) and the aerodynamics of such vehicles has much in common with those of soaring birds. Thus, much of the analysis associated with MAV development has incorporated albatross DS studies [9] or has been inspired by albatross flight [17–20]. Radio-controlled mechanical models of albatrosses have been demonstrated to exploit DS.[5] (These models are hand-launched and the energy for flight, apart from this initial boost, is extracted from the wind.)

Detailed models of albatross flight [3, 8, 9, 20] are too complicated to be transparent to non-specialists. Here we have developed a mathematical model of albatross DS that is simple and yet captures much of the underlying physics[6]. The albatross is assumed to progress by repeating a DS trajectory that is divided into three two-dimensional phases. The resulting equations of motion for each phase are very simple. Complications that are omitted (the ground effect and the influence of waves during flight phase II, and the dynamics of the turn that occurs between phase III and phase I) will aid the albatross, and so our simple model underestimates the benefits that it gains from DS. Despite these oversimplifications, our model agrees quite well with the few experimental results and observations that are available. Thus, for example, the bank angle B during turns is readily determined from the centrifugal force and weight vectors: $\tan(B) = v^2/gR$; in our model it varies between $B = 81^\circ$ and $B = 51^\circ$ for $\alpha = 0.55$–0.9. Observed bank angles are estimated to be in the range 60°–70° [20]. Looping DS trajectory in our model varies in length scale from $2R = 30$ m at $\alpha = 0.55$ to $2R = 240$ m at $\alpha = 0.9$, whereas observations from ships indicate length scales of a few hundred metres [2]. Trajectory durations of 5.0–12.7 s compare with observed durations of 9.6–10.9 s [20]. Clearly the simple model is at least compatible with observations.

[4] The turn increases energy because the bird's cross-sectional area projected along the wind direction will increase, reaching a maximum when the bird is mid-turn, and this increased area will increase the wind force acting upon the bird, so that the downwind speed at the start of phase I will exceed $v_{\min}$.

[5] See, for example, the YouTube video at http://www.youtube.com/watch?v=0rekaYTsY3I.

[6] Thus, for example, we see why albatrosses loop anticlockwise when heading north and clockwise when heading south: the prevailing winds are westerly and so the Rayleigh DS technique requires such trajectories.

References

[1] Pennycuick C J 1982 *Phil. Trans. R. Soc.* B **300** 75–106
[2] Weimerkirch H *et al* 2000 *Proc. R. Soc.* B **267** 1869–74
[3] Barnes J P 2004 How flies the Albatross *SAE International Doc.* no. 2004-01-3088
[4] Rayner J M V *et al* 2001 *Am. Zool.* **41** 188–204
[5] Pennycuick C J 2001 *J. Exp. Biol.* **204** 3283–94
[6] Tobalske B W 2007 *J. Exp. Biol.* **210** 3135–46
[7] Pennycuick C J 1989 *Bird Flight Performance: A Practical Calculation Manual* (Oxford: Oxford University Press)
[8] Wood C J 1973 *IBIS* **15** 244–56
[9] Boslough M B E 2002 Autonomous dynamic soaring platform for distributed mobile sensor arrays Sandia National Laboratories *DOE Technical Report No* SAND2002-1896
[10] Vogel S 2006 *J. Biosci.* **31** 13–25 E.g.
[11] Alexander D E and Vogel S 2002 *Nature's Flyers: Birds, Insects and the Biomechanics of Flight* (Baltimore, MD: Johns Hopkins University Press) p 62
[12] Thomson W 1883 *Nature* **27** 534–5 (Lord Rayleigh)
[13] Videler J J 2005 *Avian Flight* (Oxford: Oxford University Press) p 153
[14] Catry P, Phillips R A and Croxall J P 2004 *Auk* **121** 1208–13
[15] Withers P C and Timko P L 1977 *J. Exp. Biol.* **70** 13–26
[16] Sheng Qi-hu *et al* 2005 *Appl. Math. Mech.* **26** 1222–9
[17] Barate R *et al* 2006 *Bioinspiration Biomimetics* **1** 76–88
[18] Wharington J M 2004 Heuristic control of dynamic soaring *5th Asian Control Conf.* vol 2 pp 714–22
[19] Langelaan J W and Bramesfeld G 2008 Gust energy extraction for mini- and micro-uninhabited aerial vehicles *46th Aerosciences Conf.* American Institute of Aeronautics and Astronautics Paper 2008-0223
[20] Langelaan J W 2007 Long distance/duration trajectory optimization for small UAVs *Guidance, Navigation and Control Conf.* American Institute of Aeronautics and Astronautics Paper 2007-6737